Hindawi
Journal of Nanomaterials
Volume 2021, Article ID 6656716, 10 pages
https://doi.org/10.1155/2021/6656716

Research Article

Theoretical Study of Electronic Structure of Charged Fullerenes

Alexander Vasiliev,[1] **Leonid Matveev**,[1] **Alexander Mikhaylov**,[2] **Artem Mitrofanov**,[3] **Yuri Obukhov**,[1] **Nikita Orekhov**,[4,5] **Alexander Osadchy**,[6] **and Vladimir Stegailov**[4]

[1]*Nuclear Safety Institute of the Russian Academy of Sciences, B. Tulskaya52, 115191 Moscow, Russia*
[2]*State Scientific Center "Troitsk Institute of Innovative and Thermonuclear Investigations" (TRINITI), Pushkovykh 12, Troitsk, 108840 Moscow, Russia*
[3]*Moscow State University, Leninskiye Gory 1-2, 119991 Moscow, Russia*
[4]*Joint Institute for High Temperatures of the Russian Academy of Sciences, Izhorskaya 13, 125412 Moscow, Russia*
[5]*Bauman Moscow State Technical University, Baumanskaya 2-ya st., 5/1, 105005 Moscow, Russia*
[6]*Prokhorov General Physics Institute of the Russian Academy of Sciences, Vavilova 38, 119991 Moscow, Russia*

Correspondence should be addressed to Alexander Vasiliev; vasil@ibrae.ac.ru

Received 30 October 2020; Revised 15 March 2021; Accepted 7 April 2021; Published 4 May 2021

Academic Editor: P. Davide Cozzoli

The properties of excited short-living electron quantum levels of positively charged C_{60}^{+Z} fullerenes are numerically investigated with the help of the density functional theory (DFT) packages Quantum Espresso, ORCA, and VASP. Earlier, the existence of the volume-localized electron states for neutral and charged fullerenes was demonstrated analytically by making use of the model potential approach based on the unique quasispherical geometrical shape of C_{60}. Here, we revisit this issue by verifying numerically the existence of volume-localized states and by calculating physical parameters of all electronic states with a special focus on highly charged fullerene ions. The ionization potentials of C_{60}^{+Z} are calculated and compared with available experimental data. The photoionization cross-sections for neutral fullerene using wave functions are obtained by making use of DFT codes. We demonstrate that lifetimes of excited states vary in the range $10^{-11} \div 10^{-4}$ s, and for the volume-localized levels, lifetimes are longer than those for the surface-localized states.

1. Introduction

Much attention is attracted nowadays to the study of the new allotropic forms of carbon such as fullerenes, fullerites, onion-like fullerenes, carbon nanotubes, graphene, and doped and endohedral fullerenes [1]. It is worthwhile to mention that the existence of fullerenes as new stable carbon nanostructures had been predicted by using the Huckel method much earlier than their experimental discovery [2].

Currently, the carbon nanomaterials are considered perspective materials with applications in different technological fields. The review of physical properties and behavior of fullerenes and fullerene ions can be found, for example, in [3].

The C_{60} fullerenes (neutral ones and their ions) are very interesting and nontrivial objects from the quantum-mechanical point of view. The pairs "fullerene cation+electron" and "neutral fullerene+electron" can be viewed as the quantum coupled systems similar to an inverted nanoion $(C_{60}^{+Z} + e^{-})$ or a nanoatom if we consider $(C_{60}^{+} + e^{-})$. Recently, an experimental observation of superatom molecular orbitals (SAMO) has been reported [4–6] for neutral fullerenes. Such electronic states represent explicit examples of volume-localized electron levels (VLEL), the existence of which was theoretically analyzed in [7] and subsequently in [8–10]. To the best of our knowledge, such quantum states with the maximum of the electron density localized primarily inside fullerene's icosahedron cage of carbon atoms have not been reported before. Quantitatively, this is related to the unique geometrical form of a fullerene cluster which is very close to a sphere.

Along with these findings, the study of the electronic structure of fullerenes reveals the surface-localized electron

levels (SLEL) as typical electron states of the neutral and charged fullerenes for which the maximum of the electron density is located sharply at the (almost) spherical cage of carbon atoms. It is possible to obtain an excited VLEL or SLEL by affecting an electron beam (or light) on a fullerene ion gas. After that, the spontaneous radiative transitions from VLEL to another VLEL or to SLEL may occur in a fullerene system with a simultaneous emission of light.

Experiments demonstrate that fullerene's ionization may be as high as $Z = +10$. For example, the highly charged fullerene ions can be formed during ionization by electron beam [11], when the ions with a positive charge up to 6e per molecule were detected. In experiments with fullerenes irradiated by a jet by strong infrared laser impulse [12], stable 12-fold fullerene ions were observed (12 elementary charges per particle).

The fullerene ions can be stable or metastable. For example, numerical estimates [13] of the characteristic lifetime of the C_{60}^{+Z} ion yield the result of the order of several seconds for $Z < +11$. However, according to this study, the dramatic decrease of the fullerene ion's lifetime by 10 orders of magnitude takes place when Z increases from +11 to +13. Ion's lifetime longer than 0.5 μs was reported in the experimental study [11].

At the same time, the results of quantum-mechanical calculations based on the density functional theory (DFT) [14–16] demonstrate that the metastable fullerene ions with the degree of ionization up to $Z = +10$ can be obtained.

It is worthwhile to note that because of a large fullerene's size and its complicated geometry as compared to ordinary atoms and molecules and because of a large number of carbon atoms and electrons in a fullerene, the direct quantum-mechanical calculations for these objects are extremely complicated and are characterized by a relatively low accuracy and poor predictive power. For that reason, certain simplifying model assumptions are necessary for the qualitative and quantitative analysis of physical properties of fullerenes and their ions.

The so-called "jellium" model was successfully applied [17] to describe qualitatively the physical parameters of fullerenes observed experimentally, by calculating the energy spectrum for C_{60} as well as for C_{20} molecules and evaluating the model potential of the well and the electron wave functions for fullerene C_{60}. An idealized spherical electron gas model of a C_{60} molecule was developed to describe the optical scattering and absorption of electromagnetic wave by fullerene molecules [8]. However, the strong simplifying assumptions of the model, for example, about the electron charge density uniformly spread on the fullerene surface, affects considerably the computational accuracy of the physical characteristics of fullerene and decreases the predictive ability of the model.

The study of optical and nonlinear optical properties of fullerenes and fullerene ions with different ionization degrees Z, especially for the high values of the charge Z, attracts a lot of attention in the current research of fullerenes, onion-fullerenes, and carbon nanotubes, and it is of considerable interest both from the point of view of fundamental issues and for the future technological developments.

In this paper, we revisit the electronic structure of highly charged fullerene ions C_{60}^{+Z} with a special focus on the volume-localized quantum electron levels by making use of advanced open-source DFT codes Quantum Espresso, ORCA, and VASP.

In the next sections, we discuss the fullerene electron wave functions and the corresponding energy levels, and the photoionization cross-sections are calculated on the basis of the standard quantum-mechanical methods from the electron wave functions obtained numerically by DFT codes. The volume-localized quantum states for fullerene ions with different degree of ionization, including highly charged fullerenes, are identified, and the lifetimes of the excited levels due to radiative transitions from the excited VLELs to other VLELs and to SLELs are evaluated.

2. Methods and Approaches

In this work, we have used three modern open-source DFT codes: Quantum Espresso [18] (the program package developed in the scientific center Demokritos, Italy), ORCA [19] (the ab initio quantum chemistry program package developed by the research group of Frank Neese from Max-Planck Institute, Ruhr, Germany), and VASP [20] (the code that belongs to VASP Software GmbH, Vienna, Austria).

The above-mentioned codes were implemented to find the wave functions and the corresponding energies of the electron states for both occupied and unoccupied levels. In addition, we have developed the special numerical code which allowed us to calculate physically important parameters on the basis of wave functions and corresponding energies obtained. These parameters include the dipole-moment matrix elements of electron transitions between different states, the probability of transitions, the lifetimes of excited electronic states, and the cross-sections of different processes (photoionization, excitement of fullerene via electron collisions, recombination, etc.).

The accurate calculation of fullerene electron states is a difficult quantum-chemical task due to the size of the molecule. On the one hand, it is too big for the most accurate post-Hartree-Fock approaches [21]. Also, the region near the center of a carbon sphere may be too distinct from atoms to use gauss-type basis sets [22]. On the other hand, C_{60} is still a single molecule that casts doubt on the justification for using plane-waves approaches based on the Bloch theorem [23]. To avoid the uncertainty or method choice, we tried both plane-wave and all-electron DFT [24, 25] calculations.

Consider the methods used in our calculations in more detail. In our opinion, those options allowed to get the best modeling results. The plain wave approach was implemented into Quantum Espresso software package [18]. Electron wave functions were decomposed to a plane wave basis with energies less than 100 Ry, and Troullier-Martins norm conserving potentials were used [26]. The structure was optimized using a method based on the Broyden-Fletcher-Goldfarb-Shanno algorithm. We used supercell approach with a translation vector length of 100 a.u. nanosized materials investigation, in order to exclude interaction between fullerenes. Electron exchange and correlation were taken into account at local

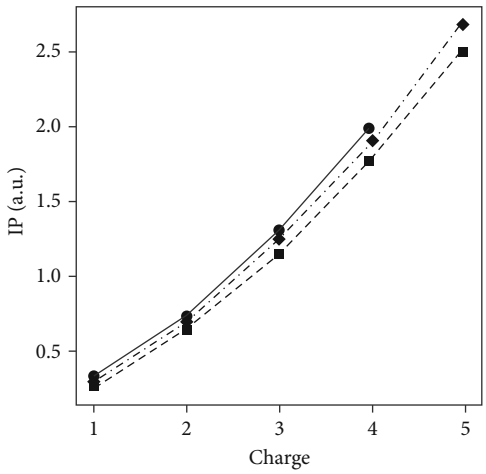

Figure 1: Fullerene's C_{60}^{+Z} ionization potentials for the charge values $Z = +1 \cdots +5$, calculated with the help of functional D3-B3LYP (dotted line, square markers) and calculated with the help of functional wb97x-d (dashed and dotted line, rhombic markers), compared with experimental data [37] (solid line, round markers).

density approximation (LDA) level in Perdew and Wang notation [27].

Pseudopotential calculations [28] were also done with projector augmented waves (PAW) [29] implemented into VASP software package [30]. An exchange-correlational term was described using generalized gradient approximation with the PBE functional [31].

All-electron calculations were done at the DFT level of theory with the ORCA package [19]. As our aim was to investigate electron states localized far from the core, we used def2-SVPD basis set with additional diffuse functions [32]. Exchange-correlation terms were included into popular hybrid functional B3LYP [33, 34], a range-separated functional wb97x-d designed to compute long-range interactions as well as short-range ones [35].

Self-consistent field procedure considers only occupied orbitals, omitting virtual ones. But the virtual orbitals are a key point of absorption/excitation process investigation. Here, the size of the molecule system prevents the use of accurate post-HF methods (as CASPT2 or especially CCSD(T)), so we have to limit ourselves to DFT approaches. On the other hand, the shape of investigated orbitals is mainly determined here by a shape of C_{60}^{+Z} potential well, i.e. quite independent to a choice of electron state with a fixed total charge.

3. Results and Discussion

In this section, we describe applications of the developed methodology to derive the physically interesting quantum-mechanical characteristics of charged fullerenes.

3.1. Ionization Potentials of Fullerene and Ions C_{60}^{+Z}. Figure 1 presents the calculated and experimental dependence ionization potential for C_{60}^{+Z} on the ionization degree Z. The results of numerical computations are obtained with the help of the code ORCA. A good agreement between the calculated and

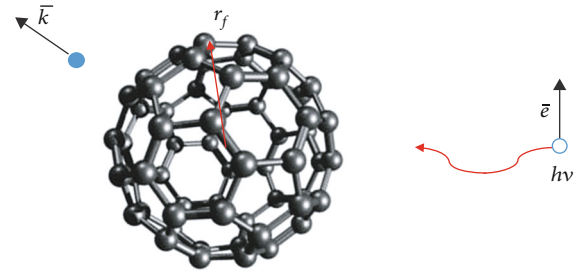

Figure 2: The geometry of fullerene photoionization problem: k is the momentum of a knocked-out electron, and e is the polarization vector of a photon with the frequency ν.

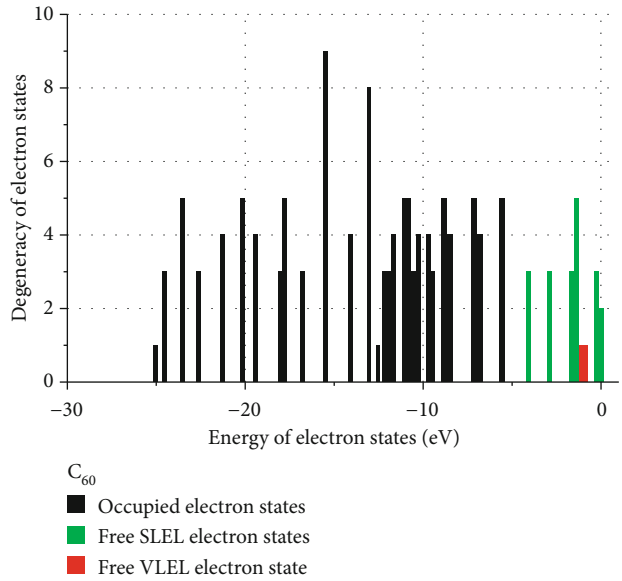

Figure 3: The density of electron states (DOS) and their degeneracy in neutral fullerene molecule on the basis of the VASP calculations: black columns—occupied SLEL electron states, green columns—free SLEL states, and red column—one free VLEL state.

experimental data is observed. The potential is shown in atomic units.

As the exact form of the functional is unknown, the choice of one of nearly two hundred of more or less widespread functionals is an essential step of modeling. Usually, the choice is based on literature data and preliminary calculations. Because the whole list is too big for detail testing, the usual convolution is based on Jacob's ladder [36]. Both of the (presented in Figure 1) functionals are from the upper steps of the ladder and proved to reproduce ionization potentials. The performance of wb97x-d may be slightly better due to included range-separated exchange that, in particular, increases accuracy for larger molecules.

3.2. Photoionization of Neutral Fullerene C_{60}. The final state of an ionized molecule C_{60} is determined by the characteristics of the knocked-out electron and the in-falling photon. One can determine the total photoionization (PI) cross-section without fixing the angle of an escaping electron. The geometry of the problem is shown in Figure 2.

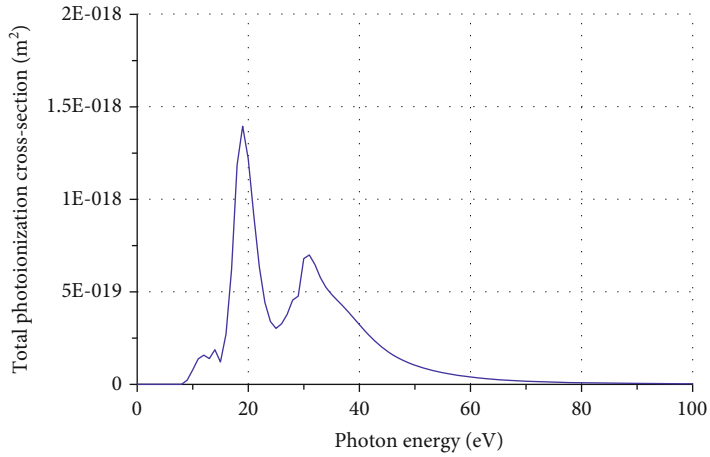

FIGURE 4: The calculated total photoionization cross-section.

We use the atomic system of units in which the reduced Planck constant, the electron charge and the electron mass are equal to unity: $h/(2\pi) = 1$, $e = 1$, $m_e = 1$. In an atomic system, the unit of length is the Bohr radius:

$$a_0 = \frac{h^2}{4\pi^2 me^2}. \quad (1)$$

Accordingly, the unit of energy in the atomic system is twice the Rydberg energy: $2\,R_y \approx 27.21$ eV.

Denoting the energy of the outgoing electron as $\varepsilon = E_n$, we have for the PI cross-section [38]

$$\sigma_n = \frac{4\pi^2}{\omega c}\int |M_{0n}|^2 \delta(E_n - E_0 - \omega)\, d\nu, \quad (2)$$

$$M_{0n} = \oint \psi_n^*(\mathbf{r})\psi_0(\mathbf{r})(\mathbf{e}\bullet\mathbf{r})\, d\mathbf{r}. \quad (3)$$

Here, ω is the energy of photon in atomic units; E_0 is the energy of an occupied electron level from which the electron is knocked out; the photon frequency is $\nu = \omega/(2\pi)$; c is the speed of light; M_{0n} is the dipole-moment matrix element; $\delta(x)$ is the delta-function. The wave functions ψ_0 and ψ_n in (2) and (3) describe the initial state (knocked-out electron) and the final state (outgoing electron), respectively, and $\mathbf{e}$ is the vector of the radiation polarization. The state ψ_n corresponds to the continuous region of spectrum.

Due to the appearance of the δ-function, equation (2) fixes the energy of the outgoing electron and determines the ionization cross-section. Namely, the energy of the outgoing electron is equal to $\varepsilon = E_0 + \omega$, and the cross-section of this process reads

$$\sigma_n = \frac{4\pi^2}{\omega c}|M_{0n}|^2. \quad (4)$$

The total PI cross-section can be obtained by taking the sum of the cross-sections (4) over all occupied electron states.

In the international unit system SI, we should multiply this value by the square of Bohr's radius:

$$a_0^2 = \left(\frac{h^2}{4\pi^2 me^2}\right)^2. \quad (5)$$

The photoionization cross-sections depend on the density of electron sates (DOS) in the fullerene. Figure 3 presents DOS of neutral fullerene calculated with the use of the VASP code. Analogous results are obtained using the ORCA code.

We calculate the dependence of the PI cross-section on the incident photon energy, represented in Figure 4, using equations (2) and (3) by making use of the wave functions which were obtained numerically with the help of the ORCA package. The characteristic peak of the PI cross-section in this graph corresponds to the photon energy of about 20 eV. This peak is well supported by the experimental data [39] (see Figure 5).

3.3. Spatial Structure of Surface- and Volume-Localized Wave Functions and Potential. Let us study the characteristic spatial structure of wave functions for highly charged fullerene ions. The 3D-structure of SLEL with the energy -8,691 eV is shown in Figure 6. We observe a very complicated shape of the electron wave function which is strongly three-dimensional (no spherical symmetry). In addition, the typical SLEL structure is manifested in the highly oscillating angular dependence of wave function amplitude (the large quantum orbital number $l >> 1$). As compared to the surface-localized states, the volume-localized typically have a low quantum orbital number $\boldsymbol{l}$, basically 0, 1, or 2. For the estimation of orbital number $\boldsymbol{l}$, we used the expression for the medium value for angular momentum operator $\widehat{\boldsymbol{l}}$ squared in the form

$$\oint dV \psi^* \widehat{l^2} \psi = l(l+1), \quad (6)$$

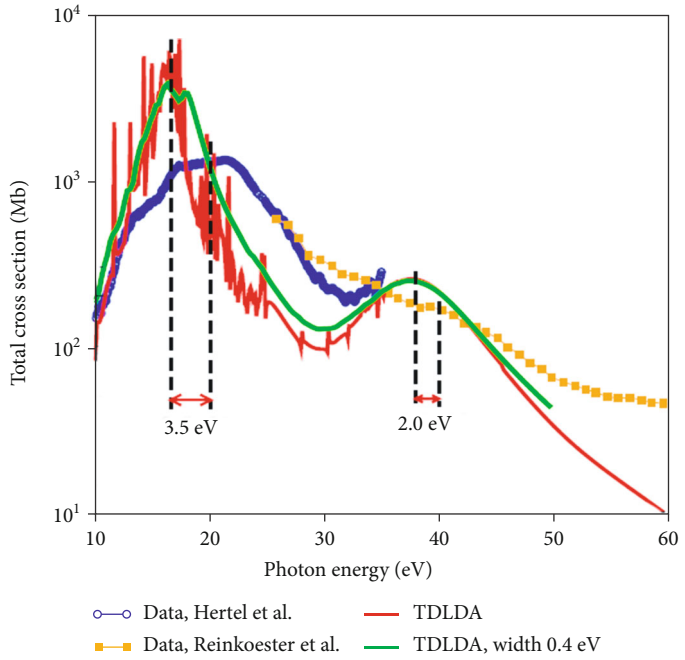

Figure 5: The calculated vs. experimental total PI cross-sections reproduced from [39]. The blue and orange curves represent the experimental data from [40, 41], respectively, and the red and green curves show the time-dependent local density approximation calculations in [39] with two different input parameters.

where ψ is the electron wave function and $\widehat{l^2} = -[(1/\sin\theta)(\partial/\partial\theta)(\sin\theta(\partial/\partial\theta)) + (1/\sin^2\theta)(\partial^2/\partial\varphi^2)]$.

Figure 7 presents the cross-section profiles of VLEL and SLEL wave functions for the C_{60}^{+10} ion. One can clearly see the difference of the spatial geometry for the volume- and surface-localized states. The wave functions of VLEL have the maximum amplitude at the center of fullerene's truncated icosahedron whereas the wave functions of SLEL are located primarily in the vicinity of the surface.

This apparent geometrical dissimilarity of the two types of electron states leads to the essential differences of the quantum-mechanical characteristics of VLELs and SLELs.

The spatial behavior of the potential for the two different ions of fullerene is shown in Figure 8. One can notice how the depth of the potential well (both at fullerene's center and at its boundary) increases with the growth of the ionization degree Z. We determine the well's depth in this statement as the difference between the lowest energy of a continuous spectrum (0 eV) and the potential in two characteristic regions (at the center and at the fullerene's sphere or its boundary). So, two potential well depths exist, respectively, shallow at the center and deep at the sphere of fullerene. One can see that both well depths get deeper with the growth of ionization degree, but the characteristic potential drop-off in the vicinity of carbon cage remains practically the same, so resulting in almost rigid shift (dependent of Z) of initial potential well to bottom.

3.4. The Lifetime of Electronic Volume-Localized and Surface-Localized States. After determining the electronic structure of the fullerene ion, i.e., the wave functions $\psi_i(\bar{r})$ corresponding to different electron states, we can evaluate the matrix elements of the electric dipole moment for an electron transition from the state i to the state k as

$$\bar{d}_{ik} = e\langle\psi_k|\bar{r}|\psi_i\rangle. \quad (7)$$

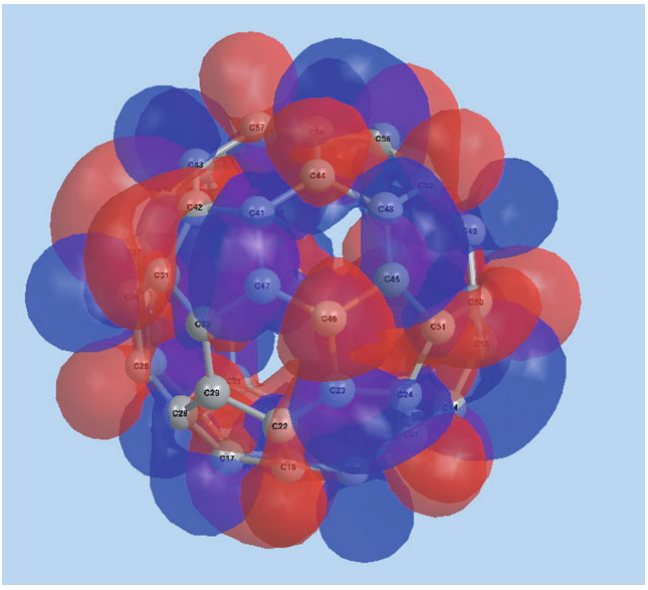

Figure 6: The 3D geometric structure of isosurfaces of wave function amplitude for C_{60}^{+3} electron state with the energy $E = -8.691$ eV. The isosurfaces are built for the energy values: 0.02 (red) and -0.02 (blue), by making use of the code Quantum Espresso.

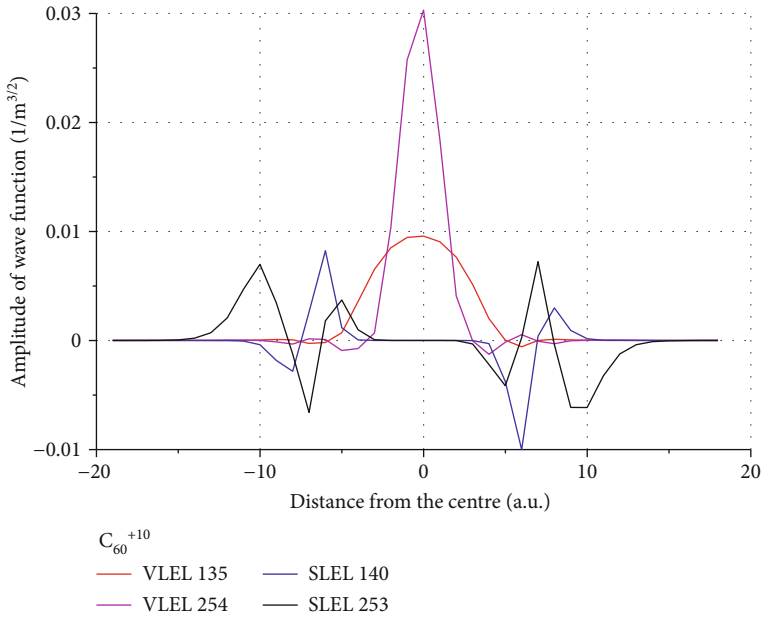

Figure 7: The cross-sections of the volume-localized and the surface-localized wave functions for C_{60}^{+10}.

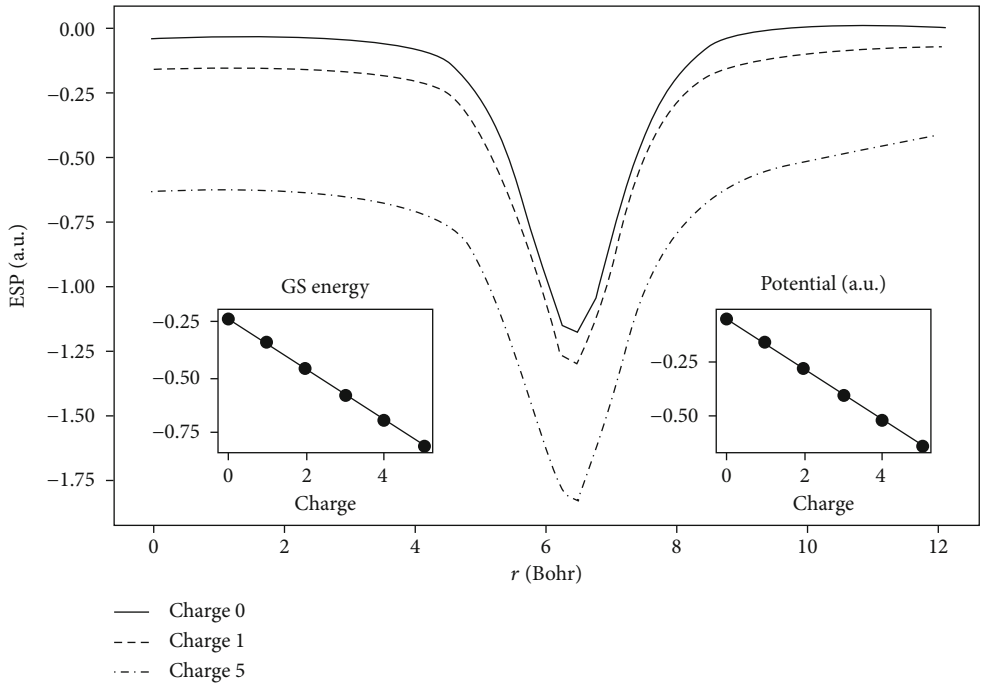

Figure 8: The profile of the potential for central cross-section of a fullerene ion C_{60}^{+Z} for charge $Z = 0, +1, +5$; the energies of the HOMO state (left small picture), and the potential in the center of the molecule (right small picture). The potentials were determined numerically with the help of the ORCA.

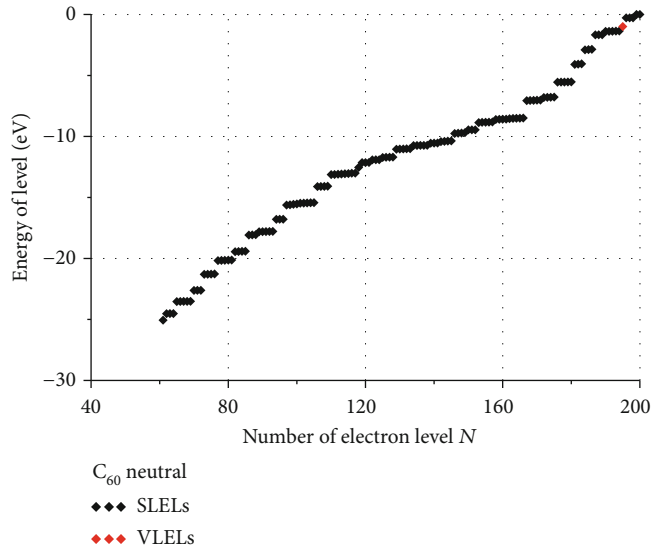

Figure 9: The energies of electron levels for neutral fullerene C_{60} numerically evaluated with the help of VASP.

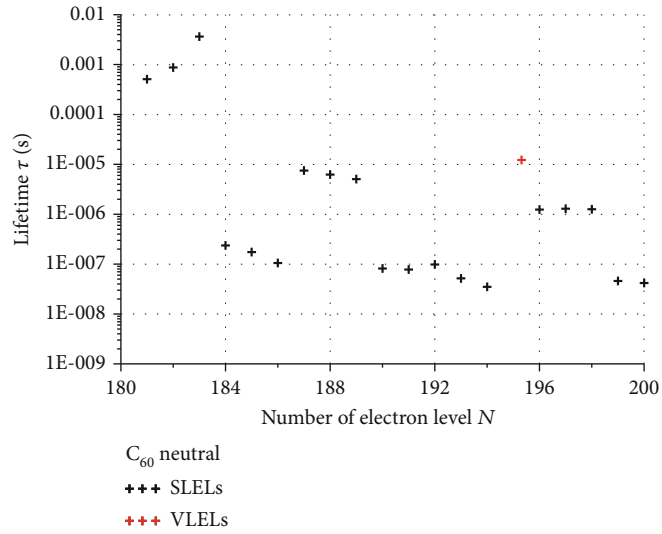

Figure 10: The lifetimes of electron levels for neutral fullerene C_{60} numerically evaluated with the help of VASP.

In Cartesian coordinates, we have

$$\bar{d}_{ik} = d_x\hat{x} + d_y\hat{y} + d_z\hat{z}. \tag{8}$$

The probability per time of spontaneous radiation via the dipole transition reads

$$P_{ik} = \frac{\omega^3}{3\pi\varepsilon_0\hbar c^3}\left|\bar{d}_{ik}\right|^2, \tag{9}$$

where

$$\hbar\omega = E_i - E_k, \left|\bar{d}_{ik}\right|^2 = d_x^2 + d_y^2 + d_z^2. \tag{10}$$

Correspondingly, the lifetime of an initial state is

$$\tau_{ik} = \frac{1}{P_{ik}}. \tag{11}$$

To calculate the lifetime for the given electron state, it is necessary to sum over the probabilities of transitions from this state to all unoccupied levels below the initial state and to take the inverse of the result.

Figure 9 presents the distribution of energies of all electron levels for a neutral fullerene C_{60}, where we calculated the energies with the help of the VASP code. Only one volume-localized electron level is discovered for a neutral fullerene; its consecutive number is 195. It appears to be the SAMO level discussed earlier in [4–6].

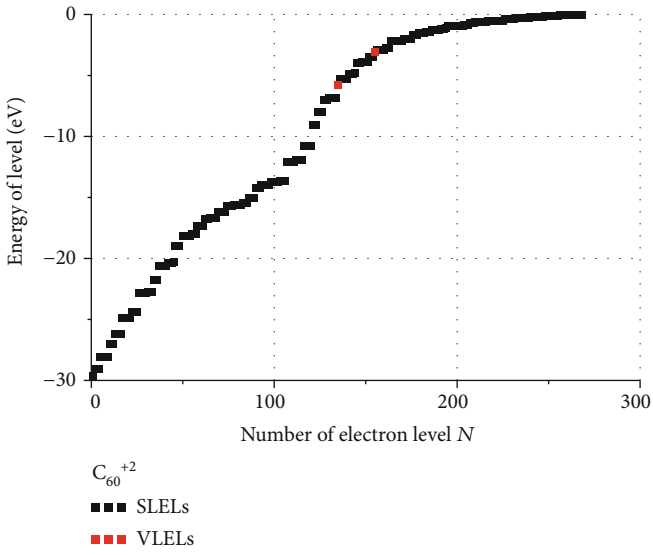

Figure 11: The energies of electron levels for the charged fullerene ion $\mathbf{C}_{60}^{+2}$ numerically evaluated with the help of the Quantum Espresso.

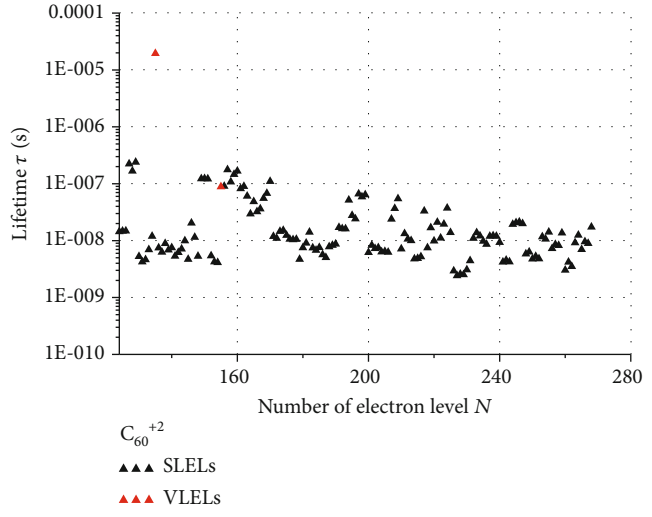

Figure 12: The lifetimes of electron levels for the charged fullerene ion $\mathbf{C}_{60}^{+2}$ numerically evaluated with the help of the Quantum Espresso.

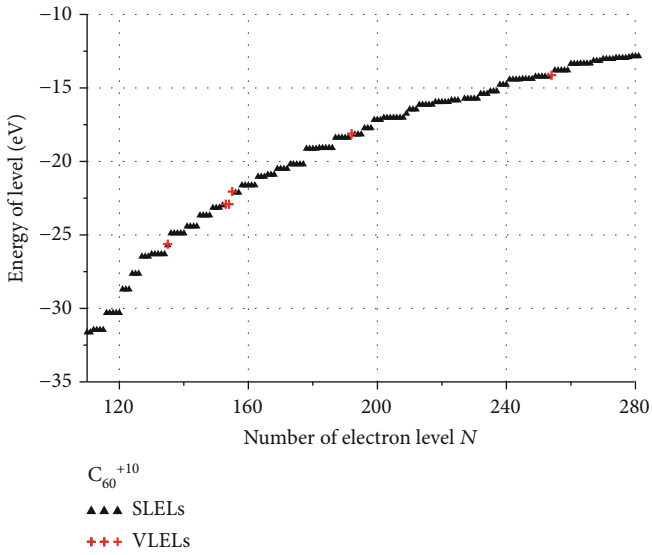

Figure 13: The energies of electron levels for fullerene ion $\mathbf{C}_{60}^{+10}$ numerically evaluated with the help of the Quantum Espresso.

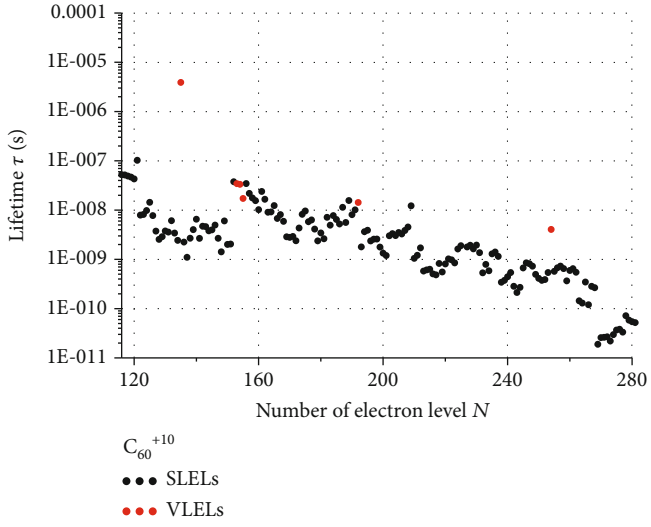

Figure 14: The lifetimes of electron levels for fullerene ion $\mathbf{C}_{60}^{+10}$ numerically evaluated with the help of the Quantum Espresso.

The lifetimes for electron levels of a neutral fullerene are depicted in Figure 10. One can see that the lifetime of the volume-localized level (#195) is much longer as compared to lifetimes of surface-localized levels with close energies.

Figure 11 shows the calculated energies for the ion $\mathbf{C}_{60}^{+2}$. For the charged fullerene, we now find two volume-localized states with the numbers 135 and 155. The corresponding lifetimes of the electronic states are presented in Figure 12, where again we observe that the lifetimes for VLELs are longer as compared to SLELs.

Next, we calculate the energies and lifetimes for the highly charged ion $\mathbf{C}_{60}^{+10}$. The corresponding numerical results are given in Figures 13 and 14, respectively. For this case, we discover six volume-localized states with the numbers 135, 153, 154, 155, 192, and 254. We therefore confirm that the number of the volume-localized states grows with the increase of the ionization degree. The physical explanation for it is as follows. The potential in the fullerene center (where VLEL has a maximum amplitude) decreases with an increase in the degree of ionization. The energy of VLELs should be located above the

potential in the center of the fullerene. Hence, the number of VLELs is expected to increase with the increase of $\boldsymbol{Z}$. In addition, we also confirm that the radiation lifetimes for VLELs are longer in comparison with SLELs (see Figure 14).

4. Conclusions

Extending the earlier results obtained in the framework of the model potential approach on the basis of the spherically symmetric approximation, in the present paper, the existence of volume-localized electron levels (VLELs) of fullerene ions C_{60}^{+Z} is demonstrated more rigorously on the basis of the detailed quantum-mechanical analysis of fullerene and its ions by making use the DFT codes Quantum Espresso, ORCA, and VASP. It is a very convincing new result which strongly supports the hypothesis about the existence of VLELs in a fullerene and its ions. The physical parameters of VLELs and SLELs, including energy and spatial structure behavior, have been obtained.

In order to verify the predictive abilities of the DFT codes used, we compared the results of computations, for a neutral fullerene and its ions, of the ionization potential as well as of the photoionization cross-sections with the experimental data available in the literature. We can conclude that the DFT codes considered in the paper are powerful numerical tools which can be successfully used for the quantum-mechanical analysis of such complicated molecules as the fullerene C_{60} and its ions. We chose the calculation options and algorithms for each code which seem to be the best one appropriate for quantum-mechanical analysis of fullerene.

We have found that the volume-localized states in general have much longer lifetimes as compared to lifetimes of the surface-localized states. This result can be explained by the relatively small values of the dipole moment matrix elements for the transitions from VLEL to SLEL due to the specific spatial structure of volume-localized wave functions. The quantum-mechanical properties of VLELs are thus essentially different from the properties of SLELs due to the different 3D geometric structures of VLELs and SLELs. As a result, the following features are confirmed:

(i) The total number of VLELs is small as compared to the total number of SLELs

(ii) The number of VLELs grows when the ionization extent of fullerene is increased

(iii) The orbital quantum number l of VLELs (as a rule 0, 1, or 2) is typically much lower as compared to that of SLELs

(iv) The lifetimes of VLELs are essentially longer in comparison with the lifetimes of SLELs

The unique features of charged fullerenes may offer new interesting practical applications including the development of new sources of coherent radiation in the wide range of wavelengths.

Data Availability

The data used to support the findings of this study are available from the corresponding author upon request.

Conflicts of Interest

The authors declare that there is no conflict of interest regarding the publication of this paper.

Acknowledgments

The authors would like to express their gratitude to the participants of the seminar of the Laboratory of Theoretical Physics at Nuclear Safety Institute and of the theoretical seminar at TRINITI, Moscow, for the valuable and stimulating discussions.

References

[1] W. H. Kroto, J. R. Heath, S. C. O'Brien, R. F. Curl, and R. E. Smalley, "C_{60}: Buckminsterfullerene," *Nature*, vol. 318, no. 6042, pp. 162-163, 1985.

[2] D. A. Bochvar and E. G. Gal'pern, "On hypothetic systems: carbon-dodehaedron s-icosahedron and carbon-s-icosahedron," *Doklady Akademii Nauk Sssr*, vol. 209, pp. 610–612, 1973.

[3] E. E. B. Campbell, *Fullerene Collision Reactions*, Kluwer Academic Publishers, Dordrecht, Netherlands, 2003.

[4] H. Li, B. Mignolet, Z. Wang et al., "Transition from SAMO to Rydberg state ionization in C60in femtosecond laser fields," *Journal of Physical Chemistry Letters*, vol. 7, no. 22, pp. 4677–4682, 2016.

[5] M. Feng, J. Zhao, and H. Petek, "Atomlike, hollow-core-bound molecular orbitals of C_{60}," *Science*, vol. 320, no. 5874, pp. 359–362, 2008.

[6] M. Feng, J. Zhao, T. Huang, X. Zhu, and H. Petek, "The electronic properties of superatom states of hollow molecules," *Accounts of Chemical Research*, vol. 44, no. 5, pp. 360–368, 2011.

[7] R. V. Arutyunyan, "Theoretical investigation of electronic properties of highly charged fullerenes. Preprint IBRAE-2018-08, Nuclear Safety Institute, Moscow," 2018, https://arxiv.org/abs/1805.08016.

[8] R. V. Arutyunyan, P. N. Vabishchevich, and Y. N. Obukhov, "Existence of a system of discrete volume-localized quantum levels for charged fullerenes," *Physical Review B*, vol. 98, no. 15, p. 155427, 2018.

[9] R. V. Arutyunyan and A. V. Osadchy, "The systems of volume-localized electron quantum levels of charged fullerenes," *Journal of Nanomaterials*, vol. 2018, Article ID 7526869, 10 pages, 2018.

[10] R. V. Arutyunyan, A. D. Vasiliev, Y. N. Obukhov, and A. V. Osadchy, "Metastable one-electron excited states of charged fullerenes," *Journal of Nanomaterials*, vol. 2019, Article ID 5864604, 4 pages, 2019.

[11] G. Senn, T. D. Mark, and P. Scheier, "Charge separation processes of highly charged fullerene ions," *The Journal of Chemical Physics*, vol. 108, no. 3, pp. 990–1000, 1998.

[12] V. R. Bhardwaj, P. B. Corkum, and D. M. Rayner, "Internal laser-induced dipole force at work inC60molecule," *Physical Review Letters*, vol. 91, no. 20, p. 203004, 2003.

[13] K. Nakai, H. Kono, Y. Sato et al., "*Ab initio* molecular dynamics and wavepacket dynamics of highly charged fullerene cations produced with intense near-infrared laser pulses," *Chemical Physics*, vol. 338, no. 2-3, pp. 127–134, 2007.

[14] M. Wierzbowska, M. Lüders, and E. Tosatti, "Multiplet structures of charged fullerenes," *Journal of Physics B: Atomic and Molecular Physics*, vol. 37, no. 13, pp. 2685–2698, 2004.

[15] S. Diaz-Tendero, M. Alcami, and F. Martin, "Coulomb stability limit of highly chargedC60q+fullerenes," *Physical Review Letters*, vol. 95, no. 1, article 013401, 2005.

[16] H. Zettergren, G. Sánchez, S. Díaz-Tendero, M. Alcamí, and F. Martín, "Theoretical study of the stability of multiply charged C_{70} fullerenes," *The Journal of Chemical Physics*, vol. 127, no. 10, p. 104308, 2007.

[17] V. K. Ivanov, G. Y. Kashenock, R. G. Polozkov, and A. V. Solov'yov, "Photoionization cross sections of the fullerenes C_{20} and C_{60} calculated in a simple spherical model," *Journal of Physics B: Atomic, Molecular and Optical Physics*, vol. 34, no. 21, pp. L669–L677, 2001.

[18] P. Giannozzi, S. Baroni, N. Bonini et al., "QUANTUM ESPRESSO: a modular and open-source software project for quantum simulations of materials," *Journal of Physics: Condensed Matter*, vol. 21, no. 39, article 395502, 2009.

[19] F. Neese, "The ORCA program system," *WIREs Computational Molecular Science*, vol. 2, no. 1, pp. 73–78, 2012.

[20] VASP, "Vienna Ab Initio Simulation Package: Atomic Scale Materials Modelling from First Principles," http://www.vasp.at/.

[21] L. González, D. Escudero, and L. Serrano-Andrés, "Progress and Challenges in the Calculation of Electronic Excited States," *ChemPhysChem*, vol. 13, no. 1, pp. 28–51, 2012.

[22] W. J. Hehre, R. F. Stewart, and J. A. Pople, "Self-Consistent Molecular-Orbital Methods. I. Use of Gaussian Expansions of Slater-Type Atomic Orbitals," *The Journal of Chemical Physics*, vol. 51, no. 6, pp. 2657–2664, 1969.

[23] F. Bloch, "Über die Quantenmechanik der Elektronen in Kristallgittern," *Zeitschrift für Physik*, vol. 52, no. 7-8, pp. 555–600, 1929.

[24] P. Hohenberg and W. Kohn, "Inhomogeneous Electron Gas," *Physical Review*, vol. 136, no. 3B, pp. B864–B871, 1964.

[25] W. Kohn and L. J. Sham, "Self-Consistent Equations Including Exchange and Correlation Effects," *Physical Review*, vol. 140, no. 4A, pp. A1133–A1138, 1965.

[26] N. Troullier and J. L. Martins, "Efficient pseudopotentials for plane-wave calculations," *Physical Review B*, vol. 43, no. 3, pp. 1993–2006, 1991.

[27] J. P. Perdew and Y. Wang, "Accurate and simple analytic representation of the electron-gas correlation energy," *Physical Review B*, vol. 45, no. 23, pp. 13244–13249, 1992.

[28] V. Heine, "The Pseudopotential Concept," *Solid State Physics*, vol. 24, pp. 1–36, 1970.

[29] P. E. Blöchl, "Projector augmented-wave method," *Physical Review B*, vol. 50, no. 24, pp. 17953–17979, 1994.

[30] G. Kresse and D. Joubert, "From ultrasoft pseudopotentials to the projector augmented-wave method," *Physical Review B*, vol. 59, no. 3, pp. 1758–1775, 1999.

[31] J. P. Perdew, K. Burke, and M. Ernzerhof, "Generalized Gradient Approximation Made Simple," *Physical Review Letters*, vol. 77, no. 18, pp. 3865–3868, 1996.

[32] F. Weigend and R. Ahlrichs, "Balanced basis sets of split valence, triple zeta valence and quadruple zeta valence quality for H to Rn: Design and assessment of accuracy," *Physical Chemistry Chemical Physics*, vol. 7, no. 18, pp. 3297–3305, 2005.

[33] K. Kim and K. D. Jordan, "Comparison of Density Functional and MP2 Calculations on the Water Monomer and Dimer," *The Journal of Physical Chemistry*, vol. 98, no. 40, pp. 10089–10094, 1994.

[34] P. J. Stephens, F. J. Devlin, C. F. Chabalowski, and M. J. Frisch, "Ab Initio Calculation of Vibrational Absorption and Circular Dichroism Spectra Using Density Functional Force Fields," *The Journal of Physical Chemistry*, vol. 98, no. 45, pp. 11623–11627, 1994.

[35] J.-D. Chai and M. Head-Gordon, "Long-range corrected hybrid density functionals with damped atom–atom dispersion corrections," *Physical Chemistry Chemical Physics*, vol. 10, no. 44, p. 6615, 2008.

[36] J. P. Perdew and K. Schmidt, "Jacob's ladder of density functional approximations for the exchange-correlation energy," in *AIP Conference Proceedings 577*, pp. 1–20, 2001.

[37] H. Deutsch, P. Scheier, K. Becker, and T. D. Mark, "A semi-empirical concept for the calculation of electron-impact ionization cross-sections of neutral and ionized fullerenes," *International Journal of Mass Spectrometry*, vol. 223-224, pp. 1–8, 2003.

[38] M. Ya, *Amusia, Atomic Photoeffect*, Plenum Press, NY, 1990.

[39] J. H. Weaver, J. L. Martins, T. Komeda et al., "Electronic structure of solid C_{60}: experiment and theory," *Physical Review Letters*, vol. 66, no. 13, pp. 1741–1744, 1991.

[40] I. V. Hertel, H. Steger, J. de Vries et al., "Giant plasmon excitation in freeC60andC70molecules studied by photoionization," *Physical Review Letters*, vol. 68, no. 6, pp. 784–787, 1992.

[41] A. Reinköster, S. Korica, G. Prümper et al., "The photoionization and fragmentation of C60in the energy range 26–130 eV," *Journal of Physics B: Atomic, Molecular and Optical Physics*, vol. 37, no. 10, pp. 2135–2144, 2004.